

Numerical modeling of a potential CO₂-supplied enhanced geothermal system (CO₂-EGS) in the Åsgard field, Norway

Maciej Miecznik¹, Magdalena Tyszer², Anna Sowizdzał³, Trond Andresen⁴, Bjørn S. Frengstad⁵, Lars A. Stenvik⁶, Karol Pierzchała⁷, Paweł Gładysz⁸

¹ Polish Academy of Sciences, Mineral and Energy Economy Research Institute, Krakow, Poland, e-mail: miecznik@min-pan.krakow.pl (corresponding author), ORCID ID: 0000-0002-6655-9814

² Polish Academy of Sciences, Mineral and Energy Economy Research Institute, Krakow, Poland, e-mail: mtyszer@min-pan.krakow.pl, ORCID ID: 0000-0002-4456-2828

³ AGH University of Krakow, Faculty of Geology, Geophysics and Environmental Protection, Krakow, Poland, e-mail: ansow@agh.edu.pl, ORCID ID: 0000-0003-1384-3763

⁴ SINTEF Energy Research, Department of Gas Technology, Trondheim, Norway, e-mail: Trond.Andresen@sintef.no, ORCID ID: 0000-0002-4730-2394

⁵ NTNU Norwegian University of Science and Technology, Department of Geoscience and Petroleum, Trondheim, Norway, e-mail: bjorn.frengstad@ntnu.no, ORCID ID: 0000-0002-1597-7282

⁶ NTNU Norwegian University of Science and Technology, Department of Geoscience and Petroleum, Trondheim, Norway; Norconsult Norge AS, Sandvika, Norway, e-mail: lars.aaberg.stenvik@norconsult.com, ORCID ID: 0000-0002-0627-8770

⁷ Polish Academy of Sciences, Mineral and Energy Economy Research Institute, Krakow, Poland, e-mail: kpierzchala@min-pan.krakow.pl, ORCID ID: 0009-0007-4976-7922

⁸ AGH University of Krakow, Faculty of Energy and Fuels, Krakow, Poland, e-mail: pawel.gladysz@agh.edu.pl, ORCID ID: 0000-0003-0219-6580

© 2024 Author(s). This is an open access publication, which can be used, distributed and re-produced in any medium according to the Creative Commons CC-BY 4.0 License requiring that the original work has been properly cited.

Received: 31 October 2023; accepted: 29 April 2024; first published online: 20 June 2024

Abstract: The principle of Enhanced Geothermal System (EGS) technology is that water injected at a sufficiently high pressure will lead to the fracturing of naturally impermeable rocks, and as a result, this will create hydraulic communication between wells. In this way, reservoirs not previously considered to be perspective can provide geothermal heat to the surface. Since nearly two decades, CO₂ is considered, mostly theoretically, as a working fluid that can potentially provide higher net power output than water in EGS's installation. In this respect, the possibility of accessing high-temperature heat from the Åre and Tilje formations located on the shelf of the Norwegian Sea was analysed. The estimated temperature at the reservoir depth of 4,500–5,000 m is not less than 165°C. For this, a 3D numerical modelling was performed in order to analyse 10 different scenarios for heat extraction using supercritical CO₂ (sCO₂) as a working fluid. Results indicate that appropriate matching of the mass flow and temperature of the injected CO₂ allows to avoid premature temperature decline in the reservoir. However, as Åre and Tilje formations are built from highly porous and relatively highly permeable rocks, the fluid entering the production well will always be a mixture of CO₂ and water. This is advantageous from the point of view that a significant part of the injected CO₂ is trapped in the reservoir, while the higher water content in the production well allows a significant temperature drop during fluid extraction to the surface to be avoided.

Keywords: EGS (Enhanced Geothermal System), CO₂-EGS, CO₂ storage, numerical modeling, TOUGH3, Åre Formation, Åsgard field

INTRODUCTION

The area of continental Norway is characterized by generally low values of terrestrial heat flux density, reaching values up to 60–70 mW/m² in the southeast of the country and along the west coast. However, the low heat flux density, low porosity and limited permeability of the crystalline bedrock have contributed to a lack of interest in the use of deep geothermal resources in Norway thus far (Kvalsvik et al. 2019, Midttømme et al. 2021). As a result, there are no conventional geothermal heating installations in mainland Norway which are producing hot thermal water from porous or fractured reservoirs. On the other hand, shallow geothermal exploitation is well developed (Midttømme et al. 2021, Nordgård-Hansen et al. 2023). The amount of heat extracted from the ground using ground-source heat pumps is estimated at around 3 TWh (10.8 PJ) annually, with a forecast of 8 TWh/a by 2030 (Sadeghi et al. 2022).

Higher values of heat flux density, and thus a higher thermal gradient, occur in the Svalbard Archipelago and the Mid-Norwegian Continental Shelf, especially in the region of the Frøya High and the Halten Terrace structural units (Slagstad et al. 2009). This area, and in particular Upper Triassic and Lower Jurassic sedimentary formations belonging to the Båt Group, deposited in deltaic and shallow marine environments, is the location of intensive hydrocarbon exploration on the Norwegian Sea. The numerous oil and gas wells have allowed for a good identification of the geological conditions and thermal parameters of the underlying formations. Measurements of temperature profiles in these wells indicate that the average geothermal gradient in this area is approximately 3.7 K/100 m, which allows temperatures of 160–170°C to be achieved at depths of ~4,700 m b.s.l., thus suitable for power production. Readers can find more information about the geological exploration and characteristics of this area in the section entitled “Geological setting”.

Taking into account the fact that Norway has extensive experience in the injection and storage of carbon dioxide in hydrocarbon formations (Furre et al. 2017), in this article the authors consider replacing water with carbon dioxide as a working fluid for receiving heat from rock

formations. Theoretical works on the use of CO₂ to obtain heat from geothermal resources began more than 20 years ago and are currently an important trend of research in the field of geothermal energy (Esteves et al. 2019, Brown 2000). As evidenced by Pruess (2006), among others, supercritical CO₂ has certain thermophysical properties that may give it an advantage over water. These include the following: low dynamic viscosity, low reactivity with reservoir rocks, as well as a strong dependence of CO₂ density on pressure and temperature, which usually permits the maintenance of the so-called the thermosiphon effect, i.e. self-maintained circulation of CO₂ between production and injection wells due to buoyance force (Pruess 2006, 2008). Moreover, Norway is pursuing an ambitious CO₂ policy, expressed, among others, by defining more radical CO₂ emission reduction targets in nationally determined contributions (NDC) concluded on the basis of the Paris Agreement (Climate Action Tracker 2022).

The issues related to the capture, transport, and mapping of areas suited for long-term and safe storage are handled by the Norwegian Offshore Directorate (NOD, former name: Norwegian Petroleum Directorate). The NOD has created a series of atlases, which consists of mapped potential of CO₂ storage on the Norwegian Shelf (Riis & Halland 2014). It shows that it is possible to store on the Norwegian Shelf more than 80 billion Mg of CO₂, of which 5.5 billion Mg of CO₂ is the estimated storage potential under the seabed of the Norwegian Sea – mostly in the Tilje and Åre formations (Halland et al. 2012). This amount (5.5 billion Mg of CO₂) is 130 times Norway’s discharge of CO₂ in 2022 (Crippa et al. 2023).

The following chapters of this article present methods and results of 3D numerical modeling of injecting supercritical carbon dioxide (sCO₂) into the combined Tilje / Åre formations in the Åsgard field, analysing the potential for heat recovery from the formation. CO₂-EGS is an innovative solution, not yet commercially used in the world, which combines energy production from EGS (Enhanced Geothermal System) and simultaneous sequestration of carbon dioxide (Sowizdżał et al. 2022). A total of 10 sCO₂ injection variants were considered, depending on the injection temperature and mass flow rate. To the authors’

knowledge, this is the first such study for this area, with the main goal to assess the possibility of using sCO₂ instead of water for heat recovery in order to generate electricity that can be used onsite on oil and gas platforms. The selected area of the Åsgard field is advantageous due to the high thermal gradient for the Tilje / Åre formations, and its selection was preceded by a detailed multivariate analysis (Pająk et al. 2021).

The EnerGizerS project internal report by Stenvik and Frengstad (2021) concluded that the Åre Formation (in combination with Tilje Formation) in the Norwegian Sea stands out as the best formation for CO₂-EGS offshore Norway, despite a relatively low rating from the cross-impact method. However, the Åre Formation possesses a high temperature (>160°C), satisfies the formation thickness criteria (>300 m), has a sealing formation above it (Ror Fm., above the Tilje Fm.) and is located close (<15 km) to multiple large oil and gas fields with relatively large emissions. An important factor in favour of this location was also the high degree of geological exploration. Alternative locations that were also considered included, among others, the Ula Formation in the North Sea and the Skagerrak Formation close to the Sleipner gas/condensate field (Stenvik & Frengstad 2021).

GEOLOGICAL SETTING

The Åre and Tilje formations in the Åsgard hydrocarbon field, located in the eastern part of the Norwegian Sea, were identified as one of the most suitable offshore regions to host the first, pilot-scale, Norwegian CO₂-EGS (Sowiżdżał et al. 2021). Seawater depth there is around 240–300 m (Fig. 1). The process of exploring geological structures with deep boreholes began there in the 1980's. In terms of geology and structure, the Åre and Tilje formations lies within the Halten Terrace, which is located on the Norwegian Continental Shelf (Fig. 2). This is a broad fault located between the Trøndelag Platform and the Møre Basin on the mid-Norwegian continental shelf (64°0'N–65°3'N). The Halten Terrace was formed as the southeastern margin of a narrow rift basin between Norway and Greenland, where the Mesozoic fault blocks of east Greenland formed the northwestern margin of the rift basin. The Halten Terrace is separated

from the Trøndelag Platform by the Bremstein Fault Zone to the east. From the west, the Halten Terrace is separated from the Møre Basin by the Klakk Fault Zone. The Vingleia Fault Zone separates the Halten Terrace from the Frøya High to the south. From the north is separated from the Dønna Terrace by the “Heidrun-Smørbukk Fault Zone” and towards the northeast narrows and continues as the strongly uplifted Nordland Ridge (Koch & Heum 1995).

Within the local model area, only four exploration boreholes with a depth of at least 4,700 m were drilled to penetrate the Early Jurassic Åre and Tilje formations (Fig. 2). In turn, the 6506/12-11 S wellbore was drilled to a measured depth of 5,268 m (MD), final true vertical depth (TVD) of 4,843 m, to be completed as a future production well. The borehole was drilled to collect data on reservoir quality and fluid distribution in the Åre and Tilje formations. Tests were also carried out in this well to examine the impact of fracking stimulation on the well's productivity (NOD 2023b).

The average thickness of the Åre Formation in the model area was assumed to be 300 m because most hydrocarbon wells do not penetrate the whole thickness of the Åre Formation. However, the estimated average thickness of the Åre Formation is between 300 and 500 m, with values increasing towards the eastern parts of the Halten Terrace, reaching a maximum thickness of 780 m in the Heidrun area (Halland et al. 2012). The Åre Formation consists of alternating sandstones and claystones interbedded with coals and coaly claystones. The Tilje Formation, lying above the Åre Formation, was deposited from Sinemurian to Pliensbachian and consists of very fine to coarse-grained sandstones interbedded with shales and siltstones. The sandstones are commonly moderately sorted with a high clay content and most beds are bioturbated. Shale clasts and coaly plant remains are common. Pure shale beds are rare, most of the finer-grained interbeds are silty or sandy (NOD 2023b). The sediments of the Ror Formation located above the Tilje Formation should act as sealing layers, preventing the migration of CO₂ upward in the rock mass (Fig. 3). The conceptual model for the 3D numerical modelling within the Åre / Tilje formations for a potential CO₂-fed enhanced geothermal system (CO₂-EGS), was established around the well 6506/12-11 S.

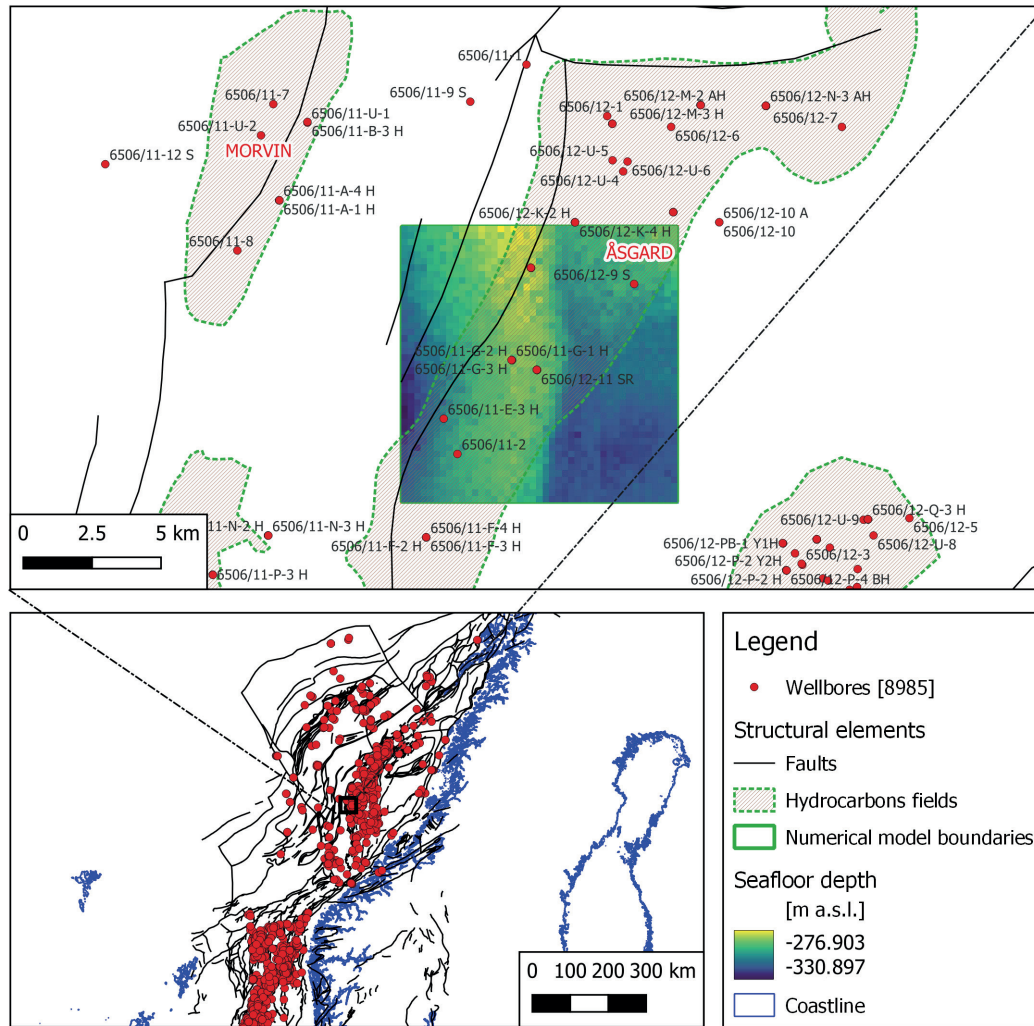


Fig. 1. Location of the numerical model of the offshore CO₂-EGS against the background of hydrocarbon fields in the Norwegian Sea and North Sea. Source: own work based on wellbore data and shapefiles accessed from the Norwegian Offshore Directorate (NOD 2023a)

The area of an assumed conceptual local model is 100 km² (10 km × 10 km) (Fig. 2). The model area was primarily selected based on the analysis of documentation from the NOD collections. The laboratory testing of core samples from these boreholes that was carried out in the EnerGizerS project was only a supplement.

The heat flow density on the territory of the Åre Formation within the Åsgard field in the area of the conceptual model is approx. 65–70 mW/m² (Slagstad et al. 2009). Based on the analysis of data from the well 6506/12-11 S, it was indicated that the geothermal gradient in the Åre Formation in this borehole, is approx. 3.35–3.86 K/100 m. The average geothermal gradient was assumed to be

3.68 K/100 m. The indicated depth for hydraulic fracturing is 4,550–4,860 m b.s.l. According to borehole data from the 6506/12-11 S wellbore, the temperature at these depths ranges from 167 to 178°C (Fig. 3).

The basic petrophysical parameters of the local rocks were mainly assessed on the basis of available drilling data. The porosity of the Båt Group (Early Jurassic deposits divided into three formations: the Åre Formation, the Tilje Formation, and the Ror Formation) of 25–35% has been reported (NOD 2023b). However, Skjæveland and Kleppe (1992) indicated that for the Tilje Formation at depths of 4,190–4,242 m, porosity amounted to 14–17%.

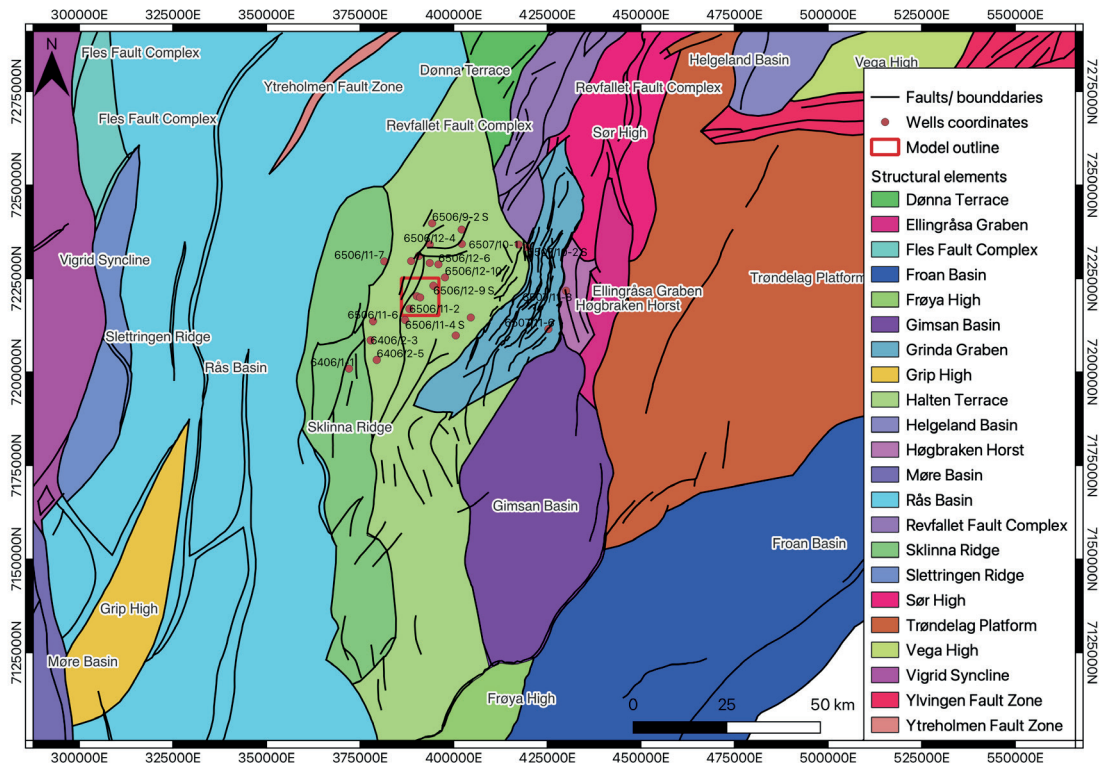


Fig. 2. Location of the local numerical model against the background of the structural elements (own work based on wellbore data and shapefiles accessed from the Norwegian Offshore Directorate – NOD 2023a)

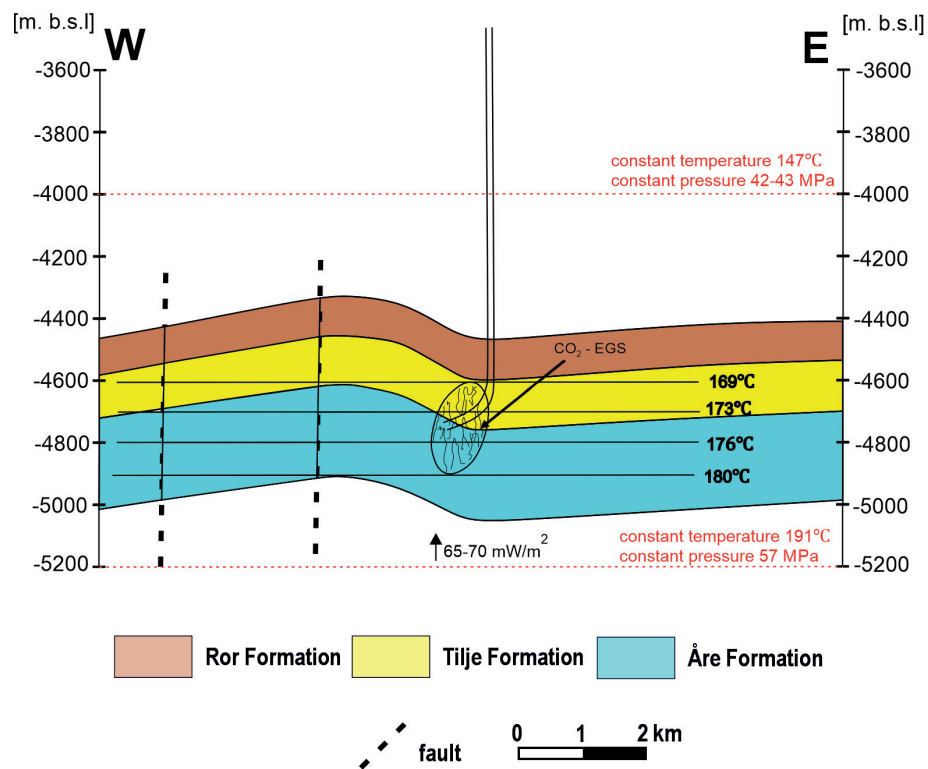


Fig. 3. A cross-section representing the conceptual model of the Åre Formation, Åsgard field (own work based on the data accessed from the Norwegian Offshore Directorate – NOD 2023a)

Therefore, rather conservative value of 15% was assumed for the numerical model. The bulk densities recorded in well logs over the territory of the local model in the Åre and Tilje formations vary from 2.17 to 2.62 g/cm³ with a mean value of 2.45 g/cm³. However, it needs to be emphasized that the bulk density values in the zone of the local model in the Åre and Tilje formations are only confirmed by three laboratory measurements, thus it is very approximate. The permeability of the Åre and Tilje formations adopted for modeling, based on borehole data, in the area of the local model was 50 millidarcys (mD) in horizontal direction and 5 mD in vertical.

METHODS

To simulate CO₂ injection into a high pressure, high temperature porous reservoir, TOUGH3 version 1.0 simulation code was used (Jung et al. 2018). TOUGH3 is primarily used for the modelling of porous and fractured geothermal reservoirs since it is able to simulate multiphase and multicomponent fluids. This software uses an integral finite difference method for space discretization, and first-order, fully implicit time differencing. A special TOUGH3 module, called ECO2N, version 2.0 (Pan et al. 2015) was used as an equation of state to simulate water, supercritical CO₂ and potentially also existence of brine in pores and fractures. ECO2N version 2.0. enables the simulation of H₂O-CO₂-NaCl mixtures in the range of up to 300°C, 800 bar and salinity up to halite saturation.

As the TOUGH3 code was written in Fortran and accepts input text files with very strict formatting, a pre- and post-processing tool was used to facilitate this time-consuming and error-prone process. This tool is a special library, called PyTOUGH (Croucher 2022), was written in the Python programming language and provides a rich set of methods for creating input files, mesh manipulation and output visualization. All of the other post-processing that PyTOUGH could not handle was performed by the authors in Python.

The main goal of this study was to simulate at least a few different scenarios with CO₂ as a working fluid, with a variable injection temperature

and flow rate to assess temperature and pressure drops between injection and production well. The output from this simulation was then used as the input for the power production analysis, using either direct CO₂ expansion turbine or the Organic Rankine Cycle. However, the power generation process is not a goal of this paper and is therefore not described here.

The fracturing of rocks occurs in a direction parallel to the maximum horizontal stress. Hence, the well trajectory should be such that its inclined/horizontal section is parallel to the direction of minimum in situ horizontal stress, as a result of which fractures propagate in a direction perpendicular to the well axis. Consequently, fractures' permeability in the radial direction to the well axis (K_r , K_z) will increase by orders of magnitude, while in the direction parallel to the well axis it will remain practically unchanged (Fig. 4). This means that the fluid flowing between the injection well and the production well will flow in a more or less straight path. This effect has a significant impact on limiting flow path tortuosity, thus limiting the heat transfer area in hard rocks with negligible natural porosity and permeability. However, in the case of the Åre and Tilje formations, it will be less significant due to the relatively high natural porosity and permeability of the deposit.

Unfortunately, due to the insufficient amount of data characterizing the geomechanical parameters of the reservoir rocks, the authors were not able to simulate the fracturing process itself. Instead of a double porosity model, a single porosity model was applied and the following assumptions were made in order to mimic an artificially fractured reservoir:

- the target depth for creating an enhanced geothermal system was set at the interval from -4,800 to -4,600 m a.s.l.;
- one injection well and one production well are separated by 1,000 m at the reservoir depth;
- the perforated intervals (working sections) of both wells are horizontal in the targeted interval at depth -4,725 m a.s.l.; each was 600 m long;
- two separate hydraulic stimulation treatments were performed from each well, resulting in creation of two zones with enhanced permeability; the half-length of newly created

fractures was assumed to be 200 m from each well axis; the height of the fractures was also assumed to be 200 m;

- hydraulic stimulation enhances permeability in direction perpendicular to well axis horizontally and vertically (in case of this particular model: Y and Z direction, respectively); there is no increase in permeability in direction along the well axis (X axis).

The 3D model has a size of 10 km × 10 km and thickness of 700 m (elevation from −5,000 to −4,300 m a.s.l.). This area is numerically represented by employing a non-uniform rectilinear grid (Fig. 5). The 3D model consists of 14 equally

thick layers of 50 m. Each layer is composed of 4,464 hexahedrons, therefore the total model consists of 62,496 blocks. The smallest blocks (50 m × 50 m) were used to increase computational precision in the area including the fractured zones and in the non-fractured zone between the injection and production wells.

Seven different rock types were distinguished in the model, representing those ranging from Early Triassic clastic deposits forming the bottom boundary of the model, to Middle Jurassic mudstones and fine-grained sandstones representing the Not Formation (belonging to the Fangst Group) in the top-most layer.

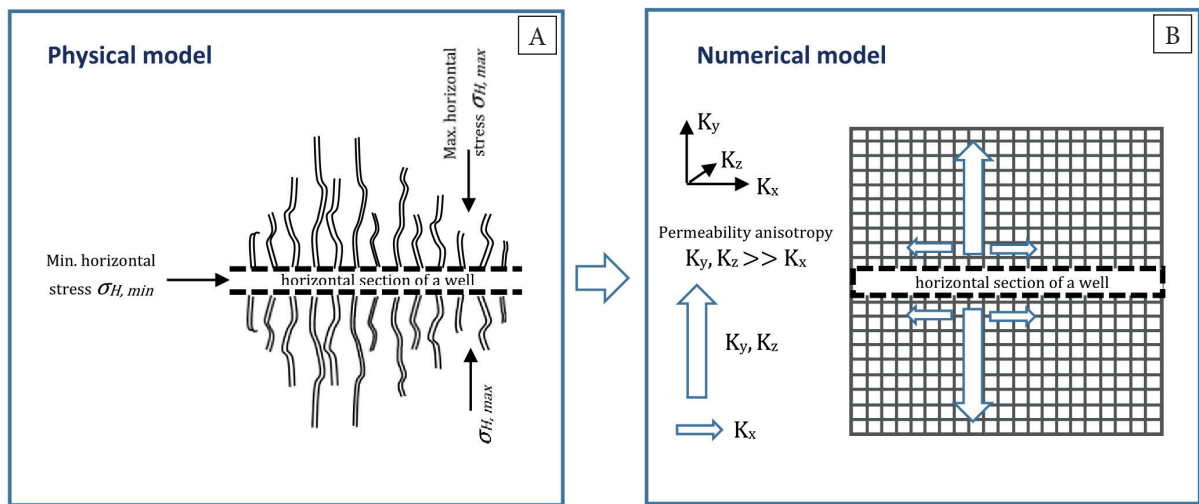


Fig. 4. Conversion from physical (A) to numerical (B) model of the fractured space; view from the top

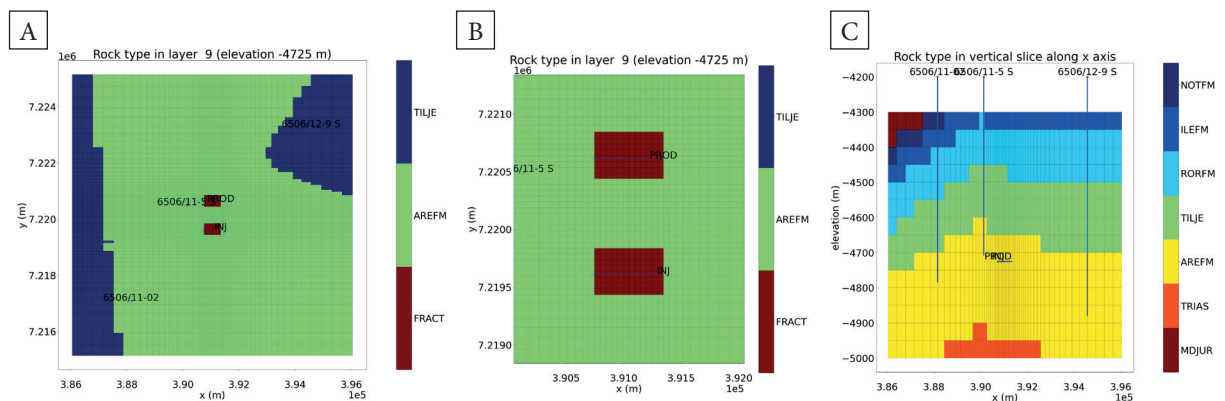


Fig. 5. Model grid: A) plane view at layer no. 9 of the grid (elevation −4,725 m a.s.l.); B) zoom of the grid to visualize better the fractured zone; C) slice view of the grid (Z scale many times exaggerated). All of the above figures are coloured according to the type of rock

Additionally, the rock type named 'FRACT' was created to represent the fractured zone in the upper part of the Åre Formation / bottom part of the Tilje Formation. The physical characteristics of these rock types are given in Table 1. Both hydrocarbon-bearing formations of the Båt Group (Tilje and Åre) were assigned the same values of petrophysical parameters. The hydraulic stimulation treatment enhanced permeability to 500 mD in Y and Z directions (two and one orders of magnitude higher, respectively, compared to the initial permeability) while keeping permeability in the direction parallel to the well axis unchanged. Due to the overall high general permeability in both the Åre and Tilje formations, high pressure buildup during fracturing is quickly released into the formation shortly after the termination of fluid injection.

The bottom-most and the top-most layer of the model are given as the constant temperature boundaries. This was done in TOUGH3 by applying unrealistically high density to these layers in order to increase their thermal inertia. On the other hand, the lateral boundaries of the model are considered as constant pressure boundaries. This was made possible by multiplying volumes of the lateral elements by a very high number in order to artificially increase fluid volume in the pores of these blocks.

The injection temperature was set at either 35°C or 50°C. The first value comes from the fact that the offshore location of the test site, with

unlimited access to cold seawater, allows the CO₂ to be cooled to approximately 10°C at the ocean floor. Moreover, the high temperature difference of CO₂ between the production and the injection well promotes the thermosyphon effect. Due to CO₂ compression effects and partly from heat transfer from the surrounding rocks, CO₂ temperature rises from about 10°C to approximately 35°C at the bottom of the injection well.

Supercritical CO₂ has a few times lower value of dynamic viscosity compared to pure water. At the formation pressure of approximately 475 bar, and a temperature of 35°C, the dynamic viscosity of CO₂ is approximately 6 times lower than the dynamic viscosity of water. For temperatures equal to the expected reservoir temperature of approximately 165°C, it is approximately 3.3 times lower for CO₂, but still significant from the point of view of the ease of fluid migration. The distance of 1,000 m between the injection and the production well was selected to limit the temperature drop in the feed zone of the production well. Shortening the distance between both wells will result in lower flow resistance, which, however, given the low dynamic viscosity of CO₂, does not seem to be as important as the delay of the cold front.

The injection of CO₂ was simulated through 12 mass source blocks along the 600-metre-long open interval of the injection well. The reservoir temperature at the depth of around 4,700 m b.s.l. is expected to be around 166°C and the assumed pressure at this depth is approximately 47.9 MPa.

Table 1

Properties of rock materials specified in the numerical model of the Tilje / Åre formations

Characteristics	Rock name							
	NOTFM	ILEFM	RORFM	TILJE	AREFM	TRIAS	MDJUR	FRACT
Description	Not Fm.	Ile Fm.	Ror Fm.	Tilje Fm.	Åre Fm.	Triassic rocks	Middle Jurassic rocks	Fractured zone
Porosity [%]	5.0	15.0	5.0	15.0	15.0	5.0	7.0	15.0
Permeability X, Y, Z [m ²]	1.0E-17	5.0E-14	1.0E-17	5.0E-14	5.0E-14	1.0E-17	1.0E-16	5.0E-14
	1.0E-17	5.0E-14	1.0E-17	5.0E-14	5.0E-14	1.0E-17	1.0E-16	5.0E-13
	1.0E-18	5.0E-15	1.0E-18	5.0E-15	5.0E-15	1.0E-18	1.0E-17	5.0E-13
Density [kg/m ³]	2,600.0							
Thermal conductivity [W/(m·K)]	1.5	2.8	1.5	2.8	2.8	1.5	1.5	2.8
Specific heat [J/(kg·K)]	900.0							

Having boundary and initial conditions specified, ten different injection / production scenarios of sCO₂ were simulated for 50 years of exploitation with a constant mass flow rate (Table 2). Of these ten scenarios, two of them were dedicated to simulate CO₂ flow in natural (not enhanced) reservoir. The remaining eight variants assume a mass flow rate from 100 to 300 kg/s and temperature of the

injected sCO₂, either 35°C or 50°C at the bottom of the injection blocks. The naming convention for the simulated scenarios is the following: M.X.Y.Z, where “X” stands for the injection / production mass flow rate, given in kilograms per second, “Y” is CO₂ injection temperature in degrees Celsius, and “Z” can be either “N” – meaning non-fractured or “F” – meaning a hydraulically fractured reservoir.

Table 2
List of simulated scenarios with a double fractured zone in Tilje / Åre formations

Characteristics	Model									
	M.200.35.N	M.200.50.N	M.100.35.F	M.100.50.F	M.150.35.F	M.150.50.F	M.200.35.F	M.200.50.F	M.300.35.F	M.300.50.F
Model domain										
Model size [m]	10,000 (X) × 10,000 (Y) × 700 (Z)									
Fractured zone size [m]	N.A.		2 × (600 × 400 × 200)							
Fractured zone volume [km ³]	N.A.		0.096							
Fractured zone permeability [m ²]	N.A. / natural permeability: X: 5.0E-14 Y: 5.0E-14 Z: 5.0E-15		X: 5.0E-14 Y: 5.0E-13 Z: 5.0E-13 + zone with natural permeability (5.0E-14, 5.0E-14, 5.0E-15) in between fractured zones							
Fractured zone porosity [-]	N.A.		0.15							
Depth of the working interval of injection and production wells [m a.s.l.]	from -4,700 to -4,750									
Distance between wells [m]	1,000									
Working length of injection and production wells [m]	600									
Orientation of the working length of injection and production wells	horizontal									
Natural temperature prior to the exploitation phase at injection / production depth [°C]	166.6									
Natural reservoir pressure outside of the fractured zone, depth = -4,725 m a.s.l. [MPa]	47.926									
Fractured zone pressure prior to the exploitation phase, but after fracturing, depth = -4,725 m a.s.l. [MPa]	47.926									
Production model variables										
Simulation time [yr]	50									
Injection / production mass flowrate [kg/s]	200	200	100	100	150	150	200	200	300	300
Injection temperature at reservoir depth [°C]	35	50	35	50	35	50	35	50	35	50

N.A. – not applicable.

RESULTS AND DISCUSSION

The results for the ten previously mentioned exploitation variants are summarized in Table 3 and presented in Figures 6–8. As it can be immediately noticed, for the same injection rate, the temperature of the injected CO₂ has a minor impact on the fluid temperature entering the production well. For the given mass flow, regardless of whether we consider artificially fractured reservoir or not, the temperature difference is less than 1°C after 50 years of constant exploitation (Fig. 6). This difference, however, could be higher for a shorter separation distance between wells or a longer time of exploitation. It is also worth paying attention to the fact that with a carbon dioxide pumping rate of 100, 150 or 200 kg/s, the temperature at the inlet to the production well remains constant for approximately 25–30 years. In case of injection rate of 300 kg/s, the cold front approaches the production well after approximately 18 years. In each case, after the cold front reaches the production well, the temperature at its inlet decreases, and the rapidity of the temperature change rate is directly proportional to the mass flow and depends only slightly on the temperature of the injected fluid (Fig. 6). A significant temperature decline ($\geq 10^\circ\text{C}$) is observed for scenarios M.300.35.F and M.300.50.F, where the temperature drop after 50 years of exploitation with constant, uninterrupted flow rate is 20.6 and 19.8°C, respectively.

The same observation regarding the injection temperature can be made in respect to the pressure difference between injection and production blocks (Fig. 7). In the analysed scenarios, injecting colder fluid did not result with the increased flow resistance. This becomes reasonable when one realizes that the ratio of dynamic viscosity to density of sCO₂ for temperatures of 35 and 50°C differs by only 8% (see Darcy Law). Of course, the higher the mass flow rate, the higher the pressure difference, but even for injection rate equal to 300 kg/s, the pressure drop in the reservoir is only 12.3–12.6 bar. Comparing the reservoir with natural permeability to the fractured one, the pressure drop is about 3.5–3.8 times higher in case of the former, for the injection rate of 200 kg/s (Table 3).

Interesting conclusions can be drawn from the analysis of Figure 8, which shows the change with time of the pore fraction occupied by CO₂ in the gaseous phase. Unlike for tight reservoirs

with low natural permeability, in the case of the Åsgard field we may expect two-phase, two-component mixture in pores. Here, the original pore fluid (i.e. water) will be dominant with respect to CO₂, as the inflow to production blocks (production well) is not solely restricted to the fractured zone. Through naturally permeable rocks, water can easily enter the production well. Simulations show that the higher the injection / production rate, the more rapid is the advent of CO₂ component to production blocks. For high mass flows (300 kg/s), the first signs of CO₂ in the produced fluid are expected to be after around 3.5 years, while for the low injection rate (100 kg/s) it is expected to happen after approximately 13 years (Fig. 8). After that time, it takes another few years to reach CO₂ saturation level at 20%. From that point, the fraction of CO₂ occupying pore volume grows less rapidly, but constantly, reaching a plateau after 30–40 years depending on the injection rate. For all cases apart from those with the lowest injection rate of 100 kg/s, the maximum saturation of CO₂ in the pore fluid is 32.5–35.0%.

Even though the temperature of the fluid entering the production well may be virtually constant for many years, a change in the CO₂ / water ratio may significantly affect thermal output of the doublet. As an example, the M.200.35.F variant was analysed further (Table 4). The dT column indicates the difference between the temperature of the fluid reaching the production well and the temperature of the injected CO₂ (35°C). The specific enthalpy of the mixture was calculated in the initial (h_{in}) and final state (h_{out}), assuming the same composition of the mixture in final and initial conditions. We believe this is the most appropriate approach because the amount of heat that one can obtain must be calculated assuming that the produced fluid is cooled back to inlet conditions. Based on this approach, a thermal output of the doublet was calculated (column dQ). The last column of Table 4 shows the ratio of the thermal output of the doublet at a given moment to the thermal output at the beginning of operation (lack of CO₂ in the production well). Comparing the first and last rows of this table, it is important to note that the temperature drop was only 0.6°C over 30 years of operation, but due to changes in the fluid composition, thermal output from the doublet decreased by 12%.

Table 3
Results for the model with a double fractured zone in the Tilje / Åre formations

Characteristics	Model no.									
	M.200.35.N	M.200.50.N	M.100.35.F	M.100.50.F	M.150.35.F	M.150.50.F	M.200.35.F	M.200.50.F	M.300.35.F	M.300.50.F
Production temperature after 30 years [°C]	165.5	165.6	166.4	166.4	166.3	166.3	165.8	165.9	160.0	160.3
Production temperature after 50 years [°C]	159.3	159.8	166.5	166.5	164.0	164.3	157.5	158.0	146.0	146.8
Pressure difference between injection and production well after 30 years [bar]	35.06	34.60	6.00	5.98	8.08	8.10	9.86	9.85	13.27	13.08
Average pressure difference between injection and production well over 50 years [bar]	33.71	33.30	5.49	5.54	7.16	7.19	8.91	8.85	12.64	12.34
Time passed to reach full CO ₂ saturation in production well [yr]	full saturation never reached									
Total CO ₂ injected in 50 years [Mg]	3.16E+08	3.16E+08	1.58E+08	1.58E+08	2.37E+08	2.37E+08	3.16E+08	3.16E+08	4.73E+08	4.73E+08
Total CO ₂ stored in rocks in 50 years [Mg]	2.32E+08	2.32E+08	1.33E+08	1.33E+08	1.81E+08	1.81E+08	2.30E+08	2.30E+08	3.30E+08	3.30E+08
Cumulative CO ₂ storage ratio after 50 years [-]	0.734	0.734	0.846	0.846	0.766	0.766	0.730	0.730	0.697	0.696
Average annual replenishment of CO ₂ from the pipeline as a result of geological storage [Mg]	4.63E+06	4.63E+06	2.67E+06	2.67E+06	3.63E+06	3.62E+06	4.61E+06	4.61E+06	6.60E+06	6.59E+06
Average daily replenishment of CO ₂ from the pipeline as a result of geological storage [Mg]	12,687.10	12,685.46	7,309.35	7,307.83	9,925.45	9,922.76	12,615.72	12,612.45	18,058.91	18,048.63

Table 4
Scenario M.200.35.F – deterioration of thermal output with changing fluid composition

Time [yr]	T _{res, out} [°C]	dT [°C]	dT _{rel} [%]	CO ₂ [vol%]	CO ₂ [mol%]	h _{in} [kJ/kg]	h _{out} [kJ/kg]	dQ [MW]	dQ _{rel} [%]
0.0	166.4	131.4	100.0	0.0	0.0	189.15	731.31	108.4	100.0
6.0	166.0	131.0	99.7	12.3	3.7	238.54	758.26	103.9	95.8
10.0	166.0	131.0	99.7	23.4	7.8	284.38	783.04	99.7	92.0
15.0	166.0	131.0	99.7	29.1	10.2	307.55	794.40	97.4	89.9
20.1	166.1	131.1	99.8	30.8	11.0	314.53	798.06	96.7	89.2
25.1	166.1	131.1	99.8	31.9	11.5	318.87	800.15	96.3	88.8
29.9	165.8	130.8	99.6	32.6	11.8	321.78	800.55	95.8	88.4

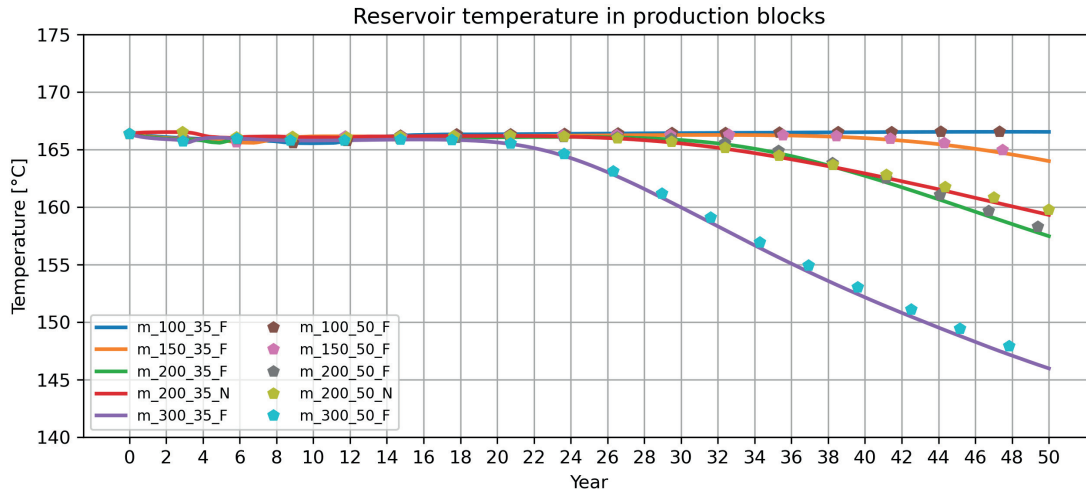


Fig. 6. Temperature variation with time for the analysed scenarios

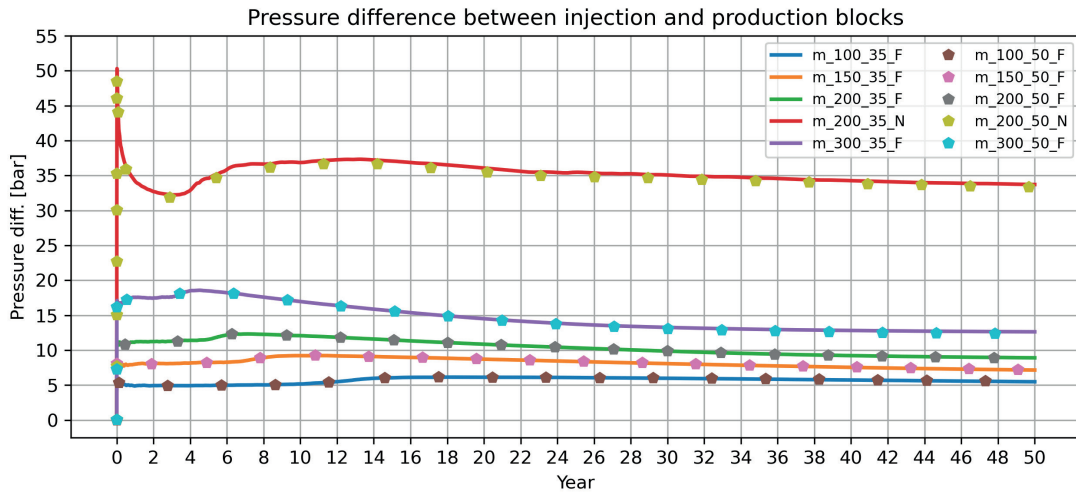


Fig. 7. Pressure difference between injection and production blocks for the analysed scenarios

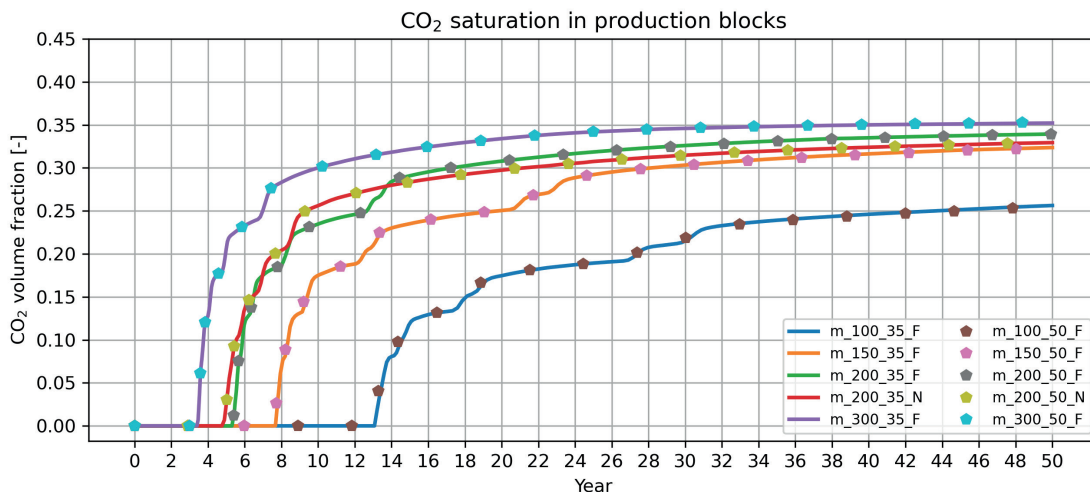


Fig. 8. Change with time of CO₂ saturation level in production blocks (by volume fraction)

This phenomenon is caused by the lower specific heat of supercritical CO₂ compared to water under the same reservoir conditions and the enthalpy of mixing that is released.

This phenomenon is not only important in terms of the thermal output at the reservoir level, but also to properly account for exergy loss in the production wellbore. Supercritical carbon dioxide expands as it moves up the well, releasing heat (losing temperature) into the rock mass much faster than water. The loss of temperature by the fluid in the wellbore is, of course, an undesirable process here, hence it is extremely important to know the fluid composition in order to accurately calculate energy capacity of each well. Apart from that, the appropriate dimensioning of the energy installation elements on the surface (fluid separators, heat exchangers, circulation pumps, transmission pipelines, etc.) requires accurate fluid composition and knowledge of its state parameters.

When we take a closer look at one of the variants, for example M.200.35.F, one can observe that for the first 6 years of operation, all of the injected CO₂ is used to fill rock pores, without being extracted. Then, the cumulative mass of CO₂ stored in the formation increases linearly with time (Fig. 9). For this particular scenario, 230 million Mg of CO₂ will be trapped in the reservoir over the course of a period of 50 years, giving an average storage rate of 4.6 million Mg annually (Table 3). The CO₂ storage ratio, that is the total amount of CO₂ stored to CO₂ injected, decreases with time and approaches a value of 73% after 50 years (Fig. 10).

We may also observe that the CO₂ plume has a diameter of approximately 2.2 km horizontally (Fig. 11), while its thickness is 500 m (Fig. 12). The Ror Formation, due to its low permeability, acts as a caprock, preventing CO₂ from migrating upward.

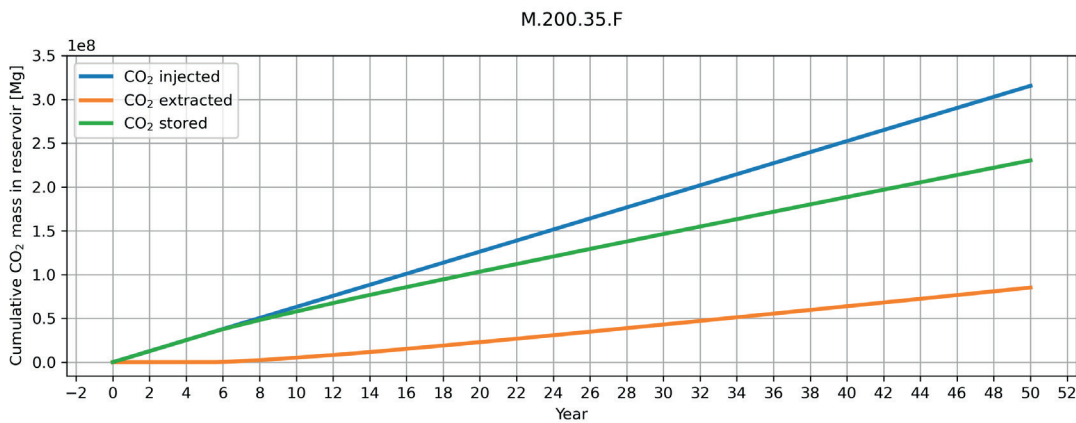


Fig. 9. The cumulative amount of CO₂ injected, stored and extracted from the reservoir

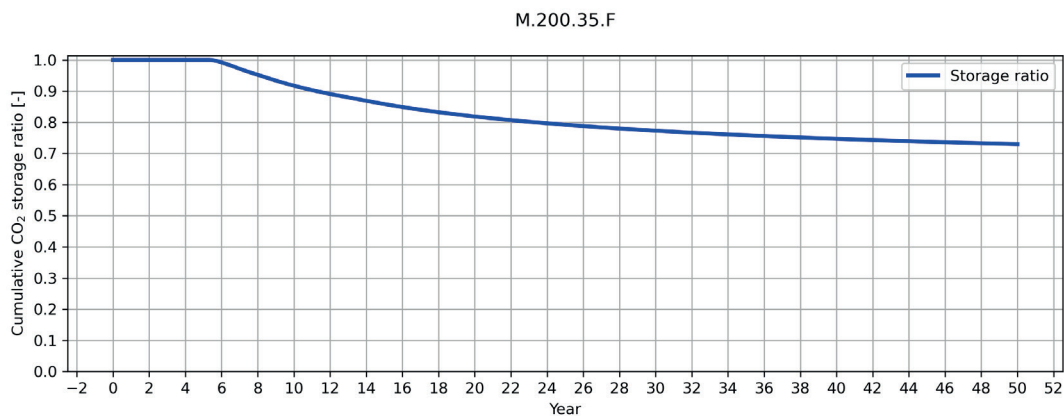


Fig. 10. The cumulative storage ratio of CO₂ in the reservoir

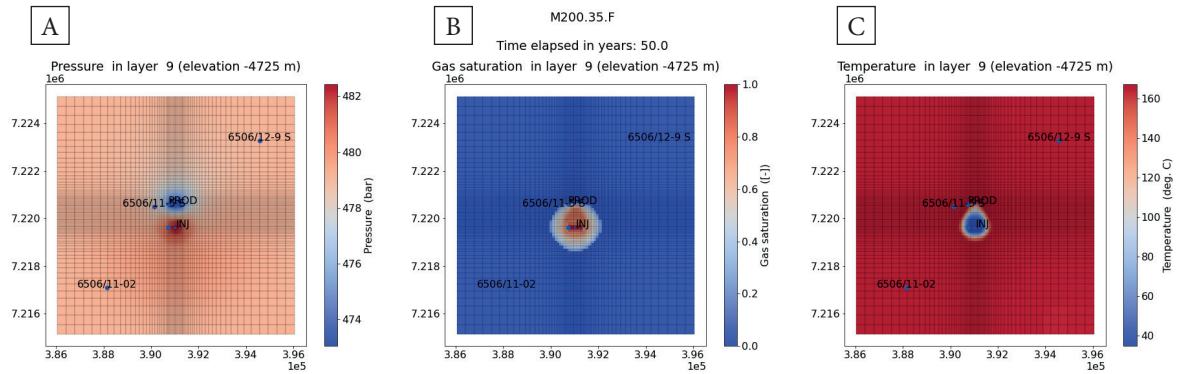


Fig. 11. Pressure (A), CO_2 gas saturation (B) and temperature (C) distribution at the depth of $-4,725$ m a.s.l. after 50 years of CO_2 -EGS constant exploitation

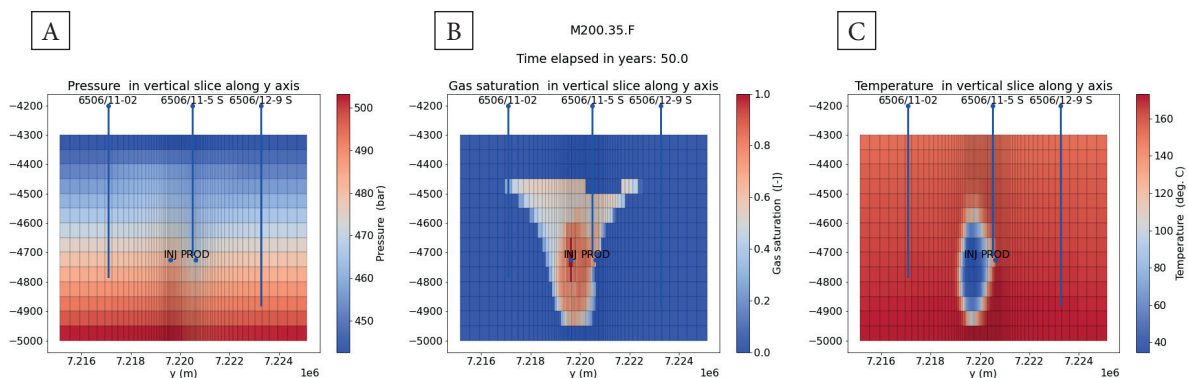


Fig. 12. Pressure (A), CO_2 gas saturation (B) and temperature (C) distribution at the cross section along the middle of the Y axis of the model, after 50 years of CO_2 -EGS constant exploitation

CONCLUSIONS

CO_2 -EGS is an interesting concept to use carbon dioxide as a working fluid to extract heat from artificially fractured rocks located at depths where the temperature is usually 150°C or more. This concept, apart from one experimental implementation in Ogachi, Japan, has not been implemented on a commercial scale. However, supercritical carbon dioxide has some thermophysical properties that compare favourably to water, such as: low dynamic viscosity and high compressibility and expansivity factor. This allows the thermosyphon effect to be attained, i.e. maintaining a higher pressure at the wellhead of the production well than the wellhead of the injection well. As a result, it is possible to maintain self-circulation between the wells, without the use of additional circulation pumps. On the other hand, supercritical carbon dioxide has an approximately 2.5 times lower specific heat value

than water. Therefore, to achieve the same thermal output from the well's doublet, a correspondingly larger mass flow of sCO_2 must be pumped. A side effect, although one beneficial from the point of view of reducing greenhouse gas emissions into the atmosphere, is the fact that a significant part of the carbon dioxide may be permanently stored in pores or structural traps.

The concept of using sCO_2 as a working fluid was applied to the Åre and Tilje formations located on the shelf of the Norwegian Sea, at depths of approximately $4,500$ – $5,000$ m b.s.l. Especially in the lower parts of the Åre Formation, below the oil and gas deposits, temperatures are expected to be high enough to consider generating electricity ($\sim 165^\circ\text{C}$ or higher). The selected rock formations are not typical for EGS reservoirs, as they are characterized by high porosity (locally up to 25–30%) and relatively high permeability (locally over 100 mD). However, fracturing operations are

also carried out in such rocks, although the extent of fractures is much more limited than in granites, for example.

The numerical modelling performed allowed us to forecast what mass flows and injection temperatures of sCO₂ permit the maintenance of a relatively small temperature drop in the reservoir. In most of the analysed scenarios, it is possible to avoid the arrival of the cold front to the production well for at least 18–20 years, which is the result of, among others, of the high volume of pores of the Tilje and Åre formations that are involved in the heat transfer, as well as a relatively large separation distance between the injection and production well (1,000 m). Because of the low dynamic viscosity of sCO₂, the pressure drops in the reservoir between injection and production well, for cases with fractured zones surrounding both wells, is between 5 and 19 bar, depending on the mass flow. In the absence of hydraulic fracturing, the increase in flow resistance may be a few times higher.

Due to high porosity, relatively high permeability, and the lack of identified sealing faults in the vicinity of both wells, the migration of naturally occurring reservoir fluids is not restricted. The results from numerical modelling indicate that, regardless of the mass flow, the fluid reaching the production well is always a mixture of sCO₂ and water, with water being the dominant component. In cases with higher flows (150–300 kg/s), the CO₂ fraction in the production well is between 30 and 35% by volume. This means, on the one hand, much lower temperature loss in the production well than in the case of CO₂ flow only, and on the other hand, the need to separate both components in the surface installation. Nevertheless, even a small share of CO₂ in a production well causes a noticeable decrease in thermal output, even maintaining the reservoir temperature unchanged. A detailed analysis of the energy conversion process, including the physical phenomena occurring in both wells, is the subject of a separate article.

The research leading to these results has received funding from the Norway Grants 2014–2021 via the National Centre for Research and Development, grant number NOR/POLNOR/EnerGizerS/0036/2019.

REFERENCES

- Brown D., 2000. A hot dry rock geothermal energy concept utilizing supercritical CO₂ instead of water. [in:] *Twenty-fifth workshop on geothermal reservoir engineering: Proceedings: Stanford University, 24–26 January 2000*, Stanford Geothermal Program, 233–238.
- Climate Action Tracker, Norway, update 1 December 2022. <https://climateactiontracker.org/countries/norway/> [access: 12.04.2024].
- Crippa M., Guizzardi D., Pagani F., Banja M., Muntean M., Schaaf E., Becker W.E., Monforti-Ferrario F., Quadrelli R., Risquez Martin A., Taghavi-Moharamli P., Köykkä J., Grassi G., Rossi S., Melo J., Oom D., Branco A., San-Miguel J. & Vignati E., 2023. *GHG emissions of all world countries – 2023*. Publications Office of the European Union, Luxembourg. <https://doi.org/10.2760/953322>.
- Croucher A., 2022. *PyTOUGH user's guide. Version 1.5.6*. Department of Engineering Science, University of Auckland, Auckland.
- Esteves A.F., Santos F.M. & Pires J.C.M., 2019. Carbon dioxide as geothermal working fluid: An overview. *Renewable and Sustainable Energy Reviews*, 114, 109331. <https://doi.org/10.1016/j.rser.2019.109331>.
- Furre A.-K., Eiken O., Alnes H., Vevatne J.N. & Kiær A.F., 2017. 20 years of monitoring CO₂-injection at Sleipner. *Energy Procedia*, 114, 3916–3926. <https://doi.org/10.1016/j.egypro.2017.03.1523>.
- Halland E.K., Johansen W.T. & Riis F. eds., 2012. *CO₂ storage atlas: Norwegian Sea*. Norwegian Petroleum Directorate, Stavanger. <https://www.sodir.no/en/whats-new/publications/co2-atlases/co2-storage-atlas-of-the-norwegian-sea/>.
- Jung Y., Shu Heng Pau G., Finsterle S. & Doughty C., 2018. *TOUGH3 User's Guide, Version 1.0*. Energy Geosciences Division, Lawrence Berkeley National Laboratory, University of California, Berkeley.
- Koch J.O. & Heum O.R., 1995. Exploration trends of the Halten Terrace. *Norwegian Petroleum Society Special Publications*, 4, 235–251. [https://doi.org/10.1016/S0928-8937\(06\)80044-5](https://doi.org/10.1016/S0928-8937(06)80044-5).
- Kvalsvik K.H., Midttømme K. & Ramstad R.K., 2019. Geothermal Energy Use, Country Update for Norway. [in:] *European Geothermal Congress 2019: The Hague, 11–14 June 2019: Proceedings*, EGEC, Brussels. <https://europeangeothermalcongress.eu/wp-content/uploads/2019/07/CUR-20-Norway.pdf>.
- Midttømme K., Alonso M.J., Krafft C.G., Kvalsvik K.H., Ramstad R.K. & Stene J., 2021. Geothermal Energy Use in Norway, Country Update for 2015–2019. [in:] *World Geothermal Congress 2020+1Reykjavik, Iceland, April 26 – May 2 2020: Proceedings*. https://www.researchgate.net/publication/340984519_Geothermal_Energy_Use_in_Norway_Country_Update_for_2015-2019.
- NOD, 2023a. *Open data*. Norwegian Offshore Directorate. <https://www.sodir.no/en/about-us/open-data/> [access: 12.03.2024].
- NOD, 2023b. *FactPages*. Norwegian Offshore Directorate. <https://factpages.sodir.no/> [access: 14.03.2024].

- Nordgård-Hansen E., Fjellså I.F., Medgyes T., Guðmundsdóttir M., Pétursson B., Miecznik M., Pająk L., Halás O., Leknes E. & Midttømme K., 2023. Differences in direct geothermal energy utilization for heating and cooling in central and northern European countries. *Energies*, 16(18), 6465. <https://doi.org/10.3390/en16186465>.
- Pająk L., Sowizdżał A., Gładysz P., Tomaszewska B., Miecznik M., Andresen T., Frengstad B.S. & Chmielowska A., 2021. Multi-criteria studies and assessment supporting the selection of locations and technologies used in CO₂-EGS Systems. *Energies*, 14(22), 7683. <https://doi.org/10.3390/en14227683>.
- Pan L., Spycher N., Doughty C. & Pruess K., 2015. *ECO2N V2.0: A TOUGH2 Fluid Property Module for Mixtures of Water, NaCl, and CO₂*. Earth Sciences Division, Lawrence Berkeley National Laboratory, University of California, Berkeley.
- Pruess K., 2006. Enhanced geothermal systems (EGS) using CO₂ as working fluid – a novel approach for generating renewable energy with simultaneous sequestration of carbon. *Geothermics*, 35(4), 351–367. <https://doi.org/10.1016/j.geothermics.2006.08.002>.
- Pruess K., 2008. On production behavior of enhanced geothermal systems with CO₂ as working fluid. *Energy Conversion & Management*, 49(6), 1446–1454. <https://doi.org/10.1016/j.enconman.2007.12.029>.
- Riis F. & Halland E., 2014. CO₂ storage atlas of the Norwegian Continental shelf: Methods used to evaluate capacity and maturity of the CO₂ storage potential. *Energy Procedia*, 63, 5258–5265. <https://doi.org/10.1016/j.egypro.2014.11.557>.
- Sadeghi H., Ijaz A. & Singh R.M., 2022. Current status of heat pumps in Norway and analysis of their performance and payback time. *Sustainable Energy Technologies and Assessments*, 54, 102829. <https://doi.org/10.1016/j.seta.2022.102829>.
- Skjæveland S. & Kleppe J., 1992. *Recent Advances in Improved Oil Recovery Methods for North Sea Sandstone Reservoirs*. SPOR Monograph, Norwegian Petroleum Directorate, Stavanger. <https://doi.org/10.13140/RG.2.1.1653.1920>.
- Slagstad T., Balling N., Elvebakk H., Midttømme K., Olesen O., Olsen L. & Pascal Ch., 2009. Heat-flow measurements in Late Palaeoproterozoic to Permian geological provinces in south and central Norway and a new heat-flow map of Fennoscandia and the Norwegian–Greenland Sea. *Tectonophysics*, 473(3–4), 341–361. <https://doi.org/10.1016/j.tecto.2009.03.007>.
- Sowizdżał A., Gładysz P., Andresen T., Miecznik M., Frengstad B.S., Liszka M., Chmielowska A., Gawron M., Løvseth S.W., Pająk L., Stenvik L. & Tomaszewska B., 2021. CO₂-enhanced geothermal systems for climate neutral energy supply. [in:] Røkke N.A. & Knuutila H.K. (eds.), *TCCS-11: The 11th International Trondheim CO₂ Capture, Transport and Storage Conference: Trondheim 22nd–23rd June 2021*, SINTEF Academic Press, Oslo, 277–283. <https://www.sintef.no/globalassets/project/tccs-11/tccs-11/sproceedings-no-7.pdf>.
- Sowizdżał A., Starczewska M. & Papiernik B., 2022. Future technology mix – enhanced geothermal system (EGS) and carbon capture, utilization, and storage (CCUS) – An overview of selected projects as an example for future investments in Poland. *Energies*, 15(10), 3505. <https://doi.org/10.3390/en15103505>.
- Stenvik L.A. & Frengstad B.S., 2021. *Geological conditions for enhanced geothermal systems with CO₂ as heat transmission fluid in Norway*. NTNU, Trondheim, Norway [unpublished report, EnerGizeS project].